

# Human Rhinovirus Attenuates the Type I Interferon Response by Disrupting Activation of Interferon Regulatory Factor 3

Tao Peng,<sup>1</sup>† Swathi Kotla,<sup>2</sup>† Roger E. Bumgarner,<sup>1</sup> and Kurt E. Gustin<sup>2\*</sup>

Department of Microbiology, School of Medicine, University of Washington,<sup>1</sup> and Department of Microbiology, Molecular Biology, and Biochemistry, University of Idaho, Moscow, Idaho 83844-3052<sup>2</sup>

Received 11 July 2005/Accepted 5 February 2006

**The type I interferon (IFN) response requires the coordinated activation of the latent transcription factors NF- $\kappa$ B, interferon regulatory factor 3 (IRF-3), and ATF-2, which in turn activate transcription from the IFN- $\beta$  promoter. Synthesis and subsequent secretion of IFN- $\beta$  activate the Jak/STAT signaling pathway, resulting in the transcriptional induction of the full spectrum of antiviral gene products. We utilized high-density microarrays to examine the transcriptional response to rhinovirus type 14 (RV14) infection in HeLa cells, with particular emphasis on the type I interferon response and production of IFN- $\beta$ . We found that, although RV14 infection results in altered levels of a wide variety of host mRNAs, induction of IFN- $\beta$  mRNA or activation of the Jak/STAT pathway is not seen. Prior work has shown, and our results have confirmed, that NF- $\kappa$ B and ATF-2 are activated following infection. Since many viruses are known to target IRF-3 to inhibit the induction of IFN- $\beta$  mRNA, we analyzed the status of IRF-3 in infected cells. IRF-3 was translocated to the nucleus and phosphorylated in RV14-infected cells. Despite this apparent activation, very little homodimerization of IRF-3 was evident following infection. Similar results in A549 lung alveolar epithelial cells demonstrated the biological relevance of these findings to RV14 pathogenesis. In addition, prior infection of cells with RV14 prevented the induction of IFN- $\beta$  mRNA following treatment with double-stranded RNA, indicating that RV14 encodes an activity that specifically inhibits this innate host defense pathway. Collectively, these results indicate that RV14 infection inhibits the host type I interferon response by interfering with IRF-3 activation.**

Rhinoviruses (RV) are small positive-stranded RNA viruses belonging to the *Picornaviridae* family. Infection by RV is most commonly associated with the development of common cold symptoms, and it is estimated that RV infections may be responsible for as many as 80% of all colds during the peak fall cold season (53). The lost productivity associated with RV infections results in an estimated loss of over 20 million work days annually in the United States alone (29). In addition, billions of dollars per year are spent in the United States on prescription and over-the-counter medicines associated with treatments for the common cold (5). RV infections have also been associated with the development of otitis media and sinusitis in children (10) and have recently been associated with the development of more-serious diseases in both the upper and lower respiratory tracts. For example, RV is commonly found in young children with pneumonia and other serious lower respiratory tract illnesses (1, 28). In fact, infections with RV are thought to be the most common cause of asthma exacerbations in young children, being identified in nearly 80% of such incidents in one study (21). RV is also frequently identified in exacerbations of chronic bronchitis and cystic fibrosis and has been isolated from immunocompromised patients with pneumonia (10, 16).

Infection with many viruses leads to the activation of innate host defense pathways that results in the production of type I

interferons (IFNs). This response requires the activation of the cellular transcription factors NF- $\kappa$ B, interferon regulatory factor 3 (IRF-3), and ATF-2, which in conjunction with the transcriptional coactivator p300/CREB binding protein (CBP) activate transcription from the IFN- $\beta$  promoter (6). Secreted IFN- $\beta$  acts in an autocrine or paracrine fashion to amplify the response by binding to the type I IFN receptor and activating the Jak/STAT signaling cascade (reviewed in reference 40). Ultimately, this results in the production of IFN- $\alpha$  and a variety of immunomodulatory and antiviral proteins, including the RNA-dependent protein kinase and 2',5'-oligoadenylate synthetase, which significantly impede viral replication.

Infection with RV results in the transcriptional induction of a number of host gene products. For example, the cell surface receptors used by major- and minor-group RV, ICAM-1 and the low density lipoprotein receptor, respectively, are upregulated following infection (35, 49). In addition, a number of proinflammatory cytokines, including granulocyte-macrophage colony-stimulating factor, interleukin-8 (IL-8), IL-6, and RANTES, are induced following infection with RV (12, 41, 47, 51, 63, 64). Work from a number of laboratories has shown that induction of these gene products is due, at least in part, to the activation of NF- $\kappa$ B, which occurs following infection (22, 34, 35, 63, 64). Recently, it was reported that infection with RV type 16 (RV16), a member of the major-group rhinoviruses, results in activation of ATF-2 and production of monocyte chemoattractant protein 1 (18). Although these results indicate that RV infection activates both NF- $\kappa$ B and ATF-2, the status of IRF-3 in RV-infected cells has not been examined.

Analysis of supernatants from RV-infected HeLa cells did not reveal the presence of significant amounts of type I inter-

\* Corresponding author. Mailing address: Department of Microbiology, Molecular Biology, and Biochemistry, University of Idaho, Moscow, Idaho 83844-3052. Phone: (208) 885-7525. Fax: (208) 885-7036. E-mail: kgustin@uidaho.edu.

† These authors contributed equally to this work.

ferons, indicating that RV infection does not elicit a strong interferon response in the host cell (46). In contrast, Wark et al. showed that infection of primary bronchial epithelial cell cultures resulted in significant production of IFN- $\beta$  (56). In addition, microarray analysis of the host transcriptional response to both RV16 and RV1B (minor group) in primary bronchial epithelial cells revealed that a variety of interferon-stimulated genes were upregulated following infection (9). Interestingly, this response could be reduced with neutralizing antibody to IFN- $\beta$ , suggesting that RV induces a type I interferon response (9). However, the observation that only 5% of the cells in these cultures were infected makes it difficult to ascertain whether these results represent the transcriptional response of infected or uninfected cells (9).

Here, using RV14 as a model serotype, we examined the type I interferon response and status of IRF-3 in infected HeLa and A549 cells. Our results indicate that RV14 infection does not induce high levels of IFN- $\beta$  mRNA or an interferon response in these cell types. We also found that IRF-3 translocates to the nucleus and appears to be phosphorylated following infection. Interestingly, however, very little IRF-3 homodimer was detected in RV-infected cells. These data suggest that RV14 infection inhibits the type I interferon response pathway by preventing the formation of functional IRF-3 complexes.

#### MATERIALS AND METHODS

**Cell culture and virus.** HeLa cells were grown in monolayer in Dulbecco's modified Eagle's medium (DMEM) supplemented with 10% fetal bovine serum, 2 mM *L*-glutamine, and penicillin-streptomycin at 37°C in 5% CO<sub>2</sub>. A549 cells, a human lung alveolar epithelial cell line, were purchased from ATCC and cultured in F-12 K medium (Invitrogen) as described above. RV14 stocks were prepared as described previously (17). Newcastle disease virus (NDV) was a gift from Chris Basler of the Mount Sinai School of Medicine. Subconfluent HeLa cells were either mock infected or infected with RV14 at a multiplicity of infection (MOI) of 50 or with NDV at an MOI of 10. Virus was adsorbed for 30 min at 32°C (RV14) or at room temperature (NDV) in phosphate-buffered saline (PBS) supplemented with 10 mM MgCl<sub>2</sub> and 10 mM CaCl<sub>2</sub> (RV14) or with 0.3% bovine serum albumin (NDV). Following adsorption, the residual virus was removed and DMEM with 10% fetal bovine serum, 2 mM *L*-glutamine, and penicillin-streptomycin was added.

**RNA isolation.** Mock-infected and infected cells were incubated at 32°C for the indicated amounts of time, and total RNA was prepared using the RNeasy midi kit (QIAGEN Inc., Valencia, Calif.) as described by the manufacturer. The quality and integrity of RNA were assessed, using denaturing agarose gel electrophoresis. For isolation of RNA from RV14-infected cells, three independent infections were performed and RNA was isolated at 1, 3, and 5 h postinfection (hpi). A single set of reference RNAs was prepared from mock-infected cells at 1-, 3-, and 5-h time points. To examine transcript levels at later times, RNA was extracted from mock- and RV14-infected HeLa cells at 7 hpi.

**Microarray analysis.** The preparation and hybridization of cRNA to Affymetrix U133A chips were performed according to the standard protocol described by Affymetrix ([www.affymetrix.com](http://www.affymetrix.com)). MAS5.0 data analysis was performed on each chip, and the results were fed to a quality control macro in Microsoft Excel to calculate the noise (average value,  $4.2 \pm 1.4$ ), the background signal level (average value,  $81.7 \pm 18.4$ ), the percent present calls (average value,  $45.7\% \pm 2.4$ ), the average signal level for all probe sets (average across all chips,  $378.5 \pm 12.6$ ), the Actin 3'/5' signal ratio (average value,  $1.08 \pm 0.08$ ), and the GAPDH (glyceraldehyde-3-phosphate dehydrogenase) 3'/5' signal ratio (average value,  $0.89 \pm 0.06$ ). Detailed quality control information for each chip is available on our supplemental website (<http://expression.washington.edu/HVEC>).

For statistical analysis, cell intensity (CEL) files were imported into the Affymetrix MAS5 program, and text files were generated for all the samples that were exported into SpotFire. The *P* value for each gene on U133A chips at 1, 3, or 5 h postinfection was generated by comparing the triplicate mock-infected samples

with the triplicate RV14-infected samples, using one-way analysis of variance (ANOVA) at each time point.

**Functional annotation of differentially expressed genes by GoMiner in the context of Gene Ontology.** The biological functions of differentially regulated genes were analyzed using GoMiner in the context of Gene Ontology (GO) (<http://discover.nci.nih.gov/gominer>). GoMiner takes as input two lists of genes: the total set on the array and the subset that the user defines as changed in expression levels. The program uses the two-sided Fisher's exact test to analyze the enrichment or depletion of a gene category in the changed-gene list relative to the number of genes that belong to the category on the U133A chip, and a *P* value is assigned to each category in the changed gene list.

**Collection and processing of published microarray data.** We have collected microarray data on cells infected with different viruses from a variety of published sources. All of the data we have collected are available at <http://expression.washington.edu/HVEC>. The following data are used in the comparison study in this paper: the Affymetrix U95A chip data from human foreskin fibroblast cells treated with IFN- $\alpha$  for 6 h (8) and human lung epithelial A549 cells infected with the A2 strain of respiratory syncytial virus (RSV) (62).

The CEL files associated with Affymetrix U95A chip data were imported into the Resolver program, the replicate samples were combined, and ratio experiments were generated. The Affymetrix Id (identifier), change (*n*-fold), and *P* value for each gene on the U95A chips were exported into SpotFire for comparison studies. To compare gene expression across array platforms, the Affymetrix Ids for all the genes in U133A and U95A gene chips were converted into a common type of gene identifier, HUGO names by MatchMiner (<http://discover.nci.nih.gov/matchminer>). Genes that belong to the GO terms, antiviral response, NF- $\kappa$ B cascade, chemokine activity, and Jak/STAT cascade were identified by GoMiner, and their expression was analyzed in SpotFire.

**Fluorescent microscopy.** HeLa cells were seeded onto 12-mm-diameter coverslips, and 24 h later the cells were transfected with an IRF-3-green fluorescent protein (GFP) expression vector (24), using Lipofectin reagent as recommended by the manufacturer (Invitrogen). After 24 h, the cells were either mock infected or infected with RV14 at an MOI of 50. The coverslips were removed at the indicated times, fixed in 3% formaldehyde for 15 min at 25°C, washed three times in PBS, and permeabilized in methanol for 5 min at -20°C. The coverslips were then washed three times in PBS, incubated in blocking solution (2% bovine serum albumin, 0.05% Triton X-100 in PBS) for 30 min at 25°C, and incubated overnight at 4°C in primary antibody against NF- $\kappa$ B/p65 (sc:109; Santa Cruz Biotechnology). The coverslips were then washed three times in blocking solution, incubated for 1 h at 25°C in secondary antibody conjugated to Alexa Fluor 555 (Molecular Probes), washed two times in PBS, stained with Hoechst 33258 (0.2  $\mu$ g/ml PBS), and mounted on glass slides with Vectashield mounting medium. The cells were viewed on a Nikon E1000M fluorescent microscope at a magnification of  $\times 100$ , and images were obtained using a Hamamatsu Orca 285 digital monochrome camera and Metamorph software (Universal Imaging).

For detection of subcellular localization of endogenous IRF-3, A549 cells were seeded onto coverslips and infected with RV14 as described above. The coverslips were removed at the indicated time points, fixed, and permeabilized in methanol-acetic acid solution (3:1) for 10 min at 25°C. IRF-3 was detected, using a rabbit polyclonal antibody (a kind gift from Takashi Fujita), and a secondary antibody was conjugated to Alexa Fluor 555 as described above.

**Quantitative real-time PCR (qRT-PCR).** The method used has been previously described (36). In brief, total RNA samples were treated with RNase-free DNase (Promega) and purified by RNeasy columns (QIAGEN). Total RNAs (1  $\mu$ g) were reverse transcribed to cDNAs using reverse transcriptase from GIBCO-BRL, and 1/40 of the total cDNA volume was used in a SYBR green PCR assay (Applied Biosystems). PCR was performed on a Bio-Rad iCycler using the following protocol: first step, 95°C for 10 min; second step, 45 cycles at 95°C for 30 s, 60°C for 30 s, and 72°C for 30 s; third step, 72°C for 5 min. The threshold cycle (*C<sub>T</sub>*) for each sample equals 10 times the standard deviation of the PCR baseline for that sample (the PCR baseline was defined as the mean values from PCR cycles 2 to 10). The *C<sub>T</sub>* differences between the controls and the treated samples (triplicates) were calculated, and the final changes (*n*-fold) in transcript levels equaled 2<sup>*x*</sup>, where *x* is the difference in *C<sub>T</sub>*. All primers were designed using the Primer 3 program found at [www.genome.wi.mit.edu](http://www.genome.wi.mit.edu) and were purchased from QIAGEN. The primer sets used for IFN- $\beta$  are 5'-ACATCCTGAGGAG ATTAAGCA-3' and 5'-GCCAGGAGTTCTCAACAATAG-3', for IL-8, 5'-ATTTCTGCAGCTCTGTGTGAAG-3' and 5'-TGTGGTCCACTCTCAATCA CTC-3', and for GAPDH, 5'-GAACATCATCCCTGCCTCTACT-3' and 5'-ATTGGCAGGTTTTTCTAGACG-3'. TaqMan rRNA control reagent (4308329; Applied Biosystems) was used for assaying the expression levels of rRNA according to the manufacturer's instructions.

**Immunoblotting.** HeLa cell lysates were prepared by scraping cells into PBS, followed by centrifugation at  $200 \times g$  for 5 min and resuspension in Tx lysis buffer (50 mM triethanolamine [pH 7.4], 500 mM NaCl, 0.5% Triton X-100, 1 mM dithiothreitol, 1 mM phenylmethylsulfonyl fluoride) containing a protease and phosphatase inhibitor cocktail (item no. 539134 [Calbiochem] and item no. P2850 [Sigma]; final concentration,  $1 \times$ ). Following 20 min of incubation on ice, the lysates were centrifuged at  $16,000 \times g$  for 5 min, and the pellet was discarded. Protein quantification was determined using the Bio-Rad protein assay kit. Equal quantities of the protein were separated on sodium dodecyl sulfate–8% polyacrylamide gel electrophoresis (PAGE) to examine ATF-2 and on 12% PAGE to examine IRF-3, followed by transfer to a polyvinylidene difluoride membrane (Millipore Corporation). Phosphorylated ATF-2 and total ATF-2 were detected using rabbit polyclonal and rabbit monoclonal antibodies, respectively (Cell Signaling). Rabbit polyclonal antibodies were used to detect IRF-3 (item no. sc-9082; Santa Cruz Biotechnology) and  $\beta$ -actin (item no. ab8227; Abcam). Mouse monoclonal antibody MS3 was used to detect nucleolin (32). Antibody-antigen complexes were detected, using a horseradish peroxidase-conjugated secondary antibody and chemiluminescence.

**IRF-3 dimerization assay.** Cell lysates were prepared by scraping cells into PBS, followed by centrifugation at  $200 \times g$  for 5 min and resuspension in native PAGE lysis buffer (50 mM Tris-Cl [pH 8.0], 150 mM NaCl, and 1% NP-40) containing a  $1 \times$  protease and phosphatase inhibitor cocktail (item no. 539134 [Calbiochem] and item no. P2850 [Sigma]). Nondenaturing 7.5% acrylamide gels were prerun at a 40-mA constant current for 30 min in cathode and anode buffer at room temperature, and equal quantities of proteins were separated at a 25-mA constant current for 50 min at  $4^\circ\text{C}$  (19). Proteins were transferred to polyvinylidene difluoride membrane membranes at a constant current of 350 mA for 1 h at  $4^\circ\text{C}$ . IRF-3 monomers and dimers were detected, using rabbit polyclonal antibody (item no. sc-9082; Santa Cruz Biotechnology), followed by a horseradish peroxidase-conjugated secondary antibody and chemiluminescence. Anti-rabbit antibody conjugated to Alexa Fluor 680 (item no. A-21076; Invitrogen) and anti-mouse antibody conjugated to IRDye 800 (item no. 610-132-121; Rockland) were used to quantify the IRF-3 monomer and dimer forms and nucleolin, respectively, on the Odyssey imager (LI-COR).

**Poly(I:C) treatment.** HeLa or A549 cells were seeded in 35-mm wells, and 24 h later, the cells were either mock infected or infected with RV14 at an MOI of 50. After 1.5 h, the cells were either treated with poly(I:C) or left untreated. For poly(I:C) treatment of HeLa cells, 100  $\mu\text{g}/\text{ml}$  of poly(I:C) (item no. P0913; Sigma) was directly added to the media. For A549 cells, 100  $\mu\text{g}/\text{ml}$  of poly(I:C) was transfected into the cells, using 800  $\mu\text{g}/\text{ml}$  of DEAE-dextran (item no. D9885; Sigma). After an additional 2.5 h of incubation, total RNA was extracted for quantitative real-time PCR or the cell lysates were prepared for immunoblot analysis.

## RESULTS

**Transcriptional profiling of HeLa cells infected with human rhinovirus type 14.** To examine the host response to RV14 infection, we prepared RNA from HeLa cells at 1, 3, 5, and 7 hpi. Reference RNAs were isolated from mock-infected cells at the same time points. RNAs were used for cRNA synthesis and hybridized to Affymetrix U133A gene chips containing 22,283 different genes, as described in Materials and Methods. All data for each time point (triplicate isolations from 1, 3, and 5 hpi, respectively) were used in one-way ANOVA to identify host cell genes that were significantly differentially expressed upon infection. For the purpose of ANOVA, the 1-, 3-, and 5-h mock-infected samples were treated as belonging to the same group; i.e., the three replicate infections for each time point were analyzed relative to the three separate mock infections. The underlying assumption in this analysis is that the gene expression patterns in the mock-infected samples are mostly unchanged relative to each other. Only one sample was prepared at 7 hpi, and consequently, it was not possible to perform ANOVA for this time point. Hence, genes were selected using the 1-, 3-, and 5-h time points, and the corresponding data for the 7-h time point is shown without an error bar. A complete list of all genes examined at each time point is provided at

TABLE 1. Identification of enriched functional categories in the set of genes affected by rhinovirus infection

GO term and time point <sup>a</sup>	Total no. of genes <sup>b</sup>	No. of down-regulated genes	No. of up-regulated genes	<i>P</i> value <sup>c</sup>
<b>RV-1 h</b>				
Transcription	1154	12	16	0.0045
Nucleus	1882	17	22	0.0111
Development	1413	9	19	0.0557
Cell cycle	543	7	6	0.0557
Protein modification	718	7	9	0.061
Signal transducer activity	1587	10	20	0.08
<b>RV-3 h</b>				
Inflammatory response	165	1	11	0.0001
Innate immune response	168	1	11	0.0001
Transcription	1154	10	23	0.006
Signal transducer activity	1587	7	34	0.0121
Humoral immune response	147	0	7	0.019
Nucleus	1882	13	33	0.0201
Development	1413	5	30	0.0373
Glycoprotein biosynthesis	71	0	4	0.0419
Apoptosis regulator activity	100	0	4	0.0994
<b>RV-5 h</b>				
Nucleus	1882	37	93	0
Transcription	1154	17	67	0.0002
Inflammatory response	165	1	17	0.0016
Innate immune response	168	1	17	0.002
RNA processing	144	7	7	0.0139
Amino acid activation	33	3	2	0.0238
Metabolism	4138	77	152	0.0243
Microtubule-associated complex	369	6	20	0.053
Apoptosis regulator activity	100	2	8	0.0292
Secretory pathway	87	2	6	0.0721

<sup>a</sup> The differentially expressed genes at each time point were annotated by GoMiner (see Materials and Methods).

<sup>b</sup> Total number of genes in the GO term that were present on U133A chips.

<sup>c</sup> GO terms that were selected with a *P* value smaller than 0.1.

<http://expression.washington.edu/HVEC>. Table 1 shows the functional categories that were enriched for differentially expressed genes in RV14-infected HeLa cells at 1, 3, and 5 hpi. At all the time points, genes assigned to the Gene Ontology terms “transcription” and “nucleus” were significantly enriched, consistent with RV14 infection resulting in significant alterations to host gene expression. By 3 hpi, several other GO terms were also enriched for differentially expressed genes, including “innate immune response” and “inflammatory response” ( $P < 0.03$ ). At 5 hpi, innate immune and inflammatory response genes were further enriched, along with several other interesting GO terms. The up-regulation of genes for the innate immune response at 3 and 5 hpi suggests that host cells respond quickly to RV14 infection. The annotation files for all the differentially expressed genes are also provided at <http://expression.washington.edu/HVEC>.

The finding that genes involved in inflammation or the innate immune response were differentially regulated following RV14 infection suggested that an antiviral response was initiated by the host cell. To further explore this possibility, we

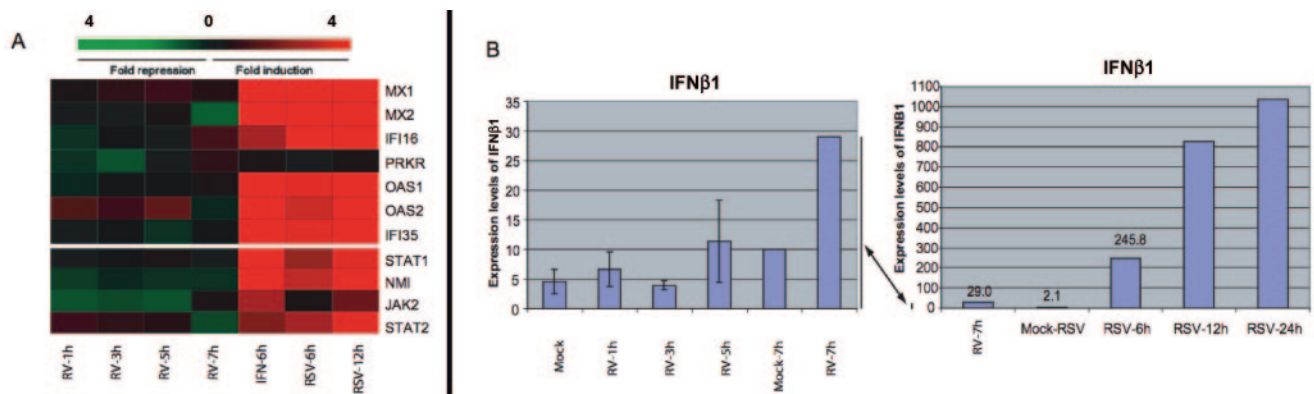


FIG. 1. RV14 infection of HeLa cells fails to induce a type I interferon response. (A) Comparison of microarray data for various ISG mRNAs from cells infected with RV14 for different periods of time (1, 3, 5, or 7 h postinfection), treated with IFN- $\alpha$  for 6 h (IFN-6h) (8), or infected with RSV for 6 h (RSV-6h) or 12 h (RSV-12h) (62). (B) Raw intensities for IFN- $\beta$  mRNA, as calculated using MAS5 analysis software, from cells infected with RV14 for 1, 3, 5, or 7 h or with RSV for 6, 12, or 24 h (62). Note that the 7-h time point for RV14-infected cells is shown in both graphs to illustrate the different levels of induction in RV14- and RSV-infected cells.

examined the status of various genes implicated in the type I interferon response pathway.

**RV14 infection fails to induce interferon- $\beta$  mRNA synthesis or activation of the Jak/STAT pathway.** Viral infection results in activation of the type I interferon response via the production of IFN- $\beta$ . Synthesis and subsequent secretion of IFN- $\beta$  then result in the activation of the Jak/STAT signal transduction cascade and activation of the full spectrum of type I IFN-stimulated genes (ISGs), thus creating an antiviral state (reviewed in reference 40). Prior work has shown that supernatants from RV14-infected HeLa cells do not provide protection against subsequent challenge with virus, indicating that infection by RV14 does not induce a strong IFN response (46). To determine if this was the case, genes known to be activated by type I interferons were examined. Figure 1A shows the host response to rhinovirus infection for several ISGs that are activated by the Jak/STAT signaling pathway. For comparison, we have included previously published data for these mRNAs obtained from cells treated with type I interferon (8). The results indicate that these ISGs were not induced following RV14 infection of HeLa cells and suggest that very little or no signaling through the Jak/STAT pathway occurs in RV14-infected cells. This is further illustrated by comparison with the transcription profiles of these genes in cells infected with RSV (62). RSV infection is known to result in the production of IFN- $\beta$  mRNA and protein and thus should activate expression of many ISGs (14, 20, 27). Analysis of the microarray data generated by Zhang et al. from RSV-infected A549 lung epithelial cells reveals that this is indeed the case (Fig. 1A) (62). This is in sharp contrast to the almost complete lack of induction of these mRNAs observed in RV14-infected HeLa cells. These results were not due to a defect in the Jak/STAT pathway in HeLa cells, as these cells are known to respond to IFN- $\alpha/\beta$  treatment (15). These results suggest either that very little IFN- $\beta$  is produced or that signaling through the Jak/STAT pathway is blocked in RV14-infected cells.

To determine if the above results could be explained by a lack of IFN- $\beta$  production, we examined the levels of IFN- $\beta$  mRNA by microarray and qRT-PCR. Figure 1B shows that the induction of IFN- $\beta$  mRNA in RV14-infected cells is barely

measurable. The intensity signals for IFN- $\beta$  mRNA were only two- to threefold greater than the background signals in all samples, indicating that RV14 failed to significantly up-regulate the expression of this mRNA. This was dramatically illustrated when we compared the IFN- $\beta$  intensity signals from RV14-infected HeLa cells with those from RSV-infected A549 cells obtained by Zhang et al. (62). Six hours following infection with RSV, the IFN- $\beta$  intensity signal was 245, and by 24 h, the signal intensity was more than 1,000. In addition to IFN- $\beta$ , there are probes corresponding to 13 different IFN- $\alpha$  mRNAs on the U133A chip, and none of these were significantly up-regulated by RV14 infection (data not shown). These results indicated that RV14 infection did not result in the transcriptional induction of IFN- $\beta$  mRNA. As many viruses are known to inhibit this response by targeting essential transcription factors such as NF- $\kappa$ B, IRF-3, and ATF-2, we focused our attention on analysis of the status of these factors in RV14-infected cells.

**Activation of IRF-3, NF- $\kappa$ B, and ATF-2 in RV14-infected HeLa cells.** Infection by many viruses results in the induction of type I interferon synthesis. This is thought to be due to the production of double-stranded RNA that in turn results in the activation of several transcription factors, including NF- $\kappa$ B, IRF-3, and ATF-2 (6). NF- $\kappa$ B and IRF-3 normally reside in the cytoplasm, but following infection by many viruses they are activated and rapidly accumulate in the nucleus (33, 60). ATF-2 is found in the nucleus at steady state, and activation requires phosphorylation on amino acids Thr69 and Thr71 (55). Following activation, these transcription factors bind to promoters of target genes and induce mRNA synthesis. To determine if RV14 might activate the type I interferon response, we examined the status of NF- $\kappa$ B, IRF-3, and ATF-2 in infected cells. Figure 2A shows that, as expected, NF- $\kappa$ B and IRF-3 were cytoplasmic in mock-infected cells and that this had not changed by 1.5 hpi. By 3 hpi postinfection, IRF-3 was predominantly nuclear, suggesting that it was activated following infection with RV14. Similarly, NF- $\kappa$ B was also translocated to the nuclei of cells by 3 hpi (Fig. 2A). This observation is in agreement with numerous reports that NF- $\kappa$ B is activated following rhinovirus infection (22, 34, 35, 63, 64).

To examine ATF-2 activation, we utilized a phospho-specific

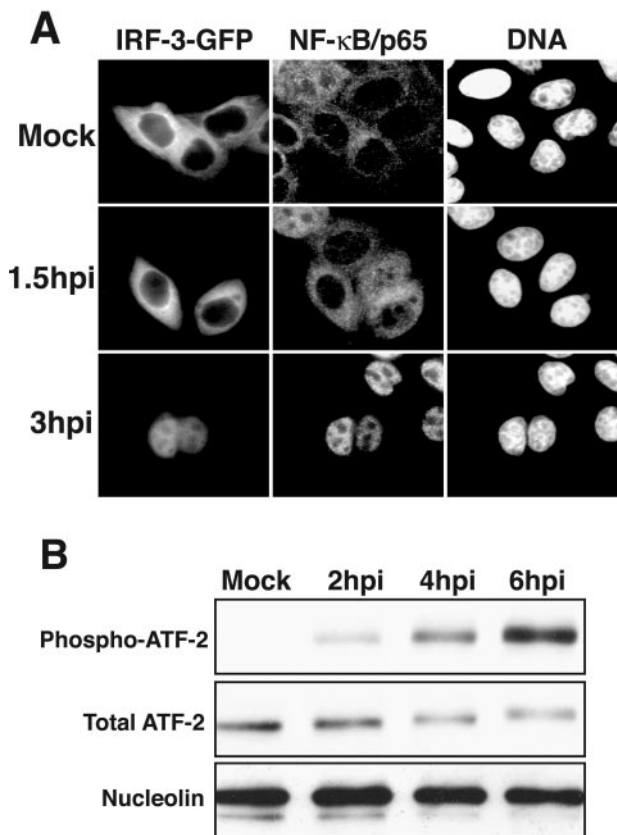


FIG. 2. Activation of NF- $\kappa$ B, IRF-3, and ATF-2 in RV14-infected cells. (A) Nuclear accumulation of IRF-3 and NF- $\kappa$ B. HeLa cells were transiently transfected with an IRF-3-GFP expression vector and were either mock infected or infected with RV14 and analyzed at 1.5 or 3 hpi. The panels labeled IRF-3-GFP show the localization of the IRF-3-GFP fusion protein, using a fluorescein isothiocyanate filter. The NF- $\kappa$ B/p65 panels show the same field stained with antibodies to detect the p65 subunit of NF- $\kappa$ B, visualized using a tetramethyl rhodamine isothiocyanate filter. The DNA panels show the same field stained with Hoechst to reveal cell nuclei. (B) Phosphorylation of ATF-2. Whole-cell lysates (25  $\mu$ g) prepared from mock-infected cells or cells that had been infected for the indicated amounts of time were analyzed by immunoblotting. ATF-2 was detected by sequentially probing the membrane, using antibodies that recognize the phosphorylated form of ATF-2 (phospho-ATF-2) and all forms of ATF-2 (Total ATF-2). The membrane was also probed with an antibody to nucleolin to show equivalent loading of protein lysates.

antibody that reacts only with activated ATF-2. As expected, very little phospho-ATF-2 was present in mock-infected cells, consistent with ATF-2 being in an inactivated state (Fig. 2B). Two hours after infection with RV14, phospho-ATF-2 was readily detected, and the levels continued to increase from 4 to 6 hpi (Fig. 2B). This was not due to an overall increase in ATF-2 protein levels, as the total amount of ATF-2 present in RV14-infected cells did not increase (Fig. 2B). These findings are in agreement with a recent report showing that infection with RV16 results in the activation of ATF-2 (18). In summary, these results suggest an interesting observation: that RV14 infection results in the activation of NF- $\kappa$ B, IRF-3, and ATF-2 without detectable levels of IFN- $\beta$  mRNA.

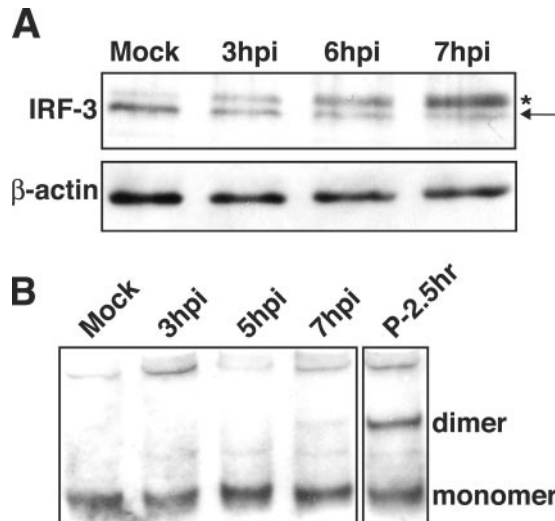


FIG. 3. Phosphorylation and homodimerization of IRF-3 in HeLa cells. (A) Phosphorylation of IRF-3. Whole-cell lysates prepared from mock-infected cells or cells that had been infected with RV14 for the indicated amounts of time were analyzed by immunoblotting. IRF-3 was detected by probing the membrane with rabbit polyclonal antibody that detects IRF-3. The nonphosphorylated form of IRF-3 is indicated with an arrow, and the phosphorylated form is indicated with an asterisk. The membrane was stripped and reprobed with an antibody to  $\beta$ -actin to show equivalent loading of protein. (B) Homodimerization of IRF-3. Cell lysates prepared from mock-infected cells or cells that had been infected with RV14 or treated with poly(I:C) for the indicated amounts of time were analyzed by native PAGE, followed by immunoblotting to detect IRF-3. The monomeric and dimeric forms of IRF-3 are indicated.

**Phosphorylation and dimerization of IRF-3.** IRF-3 plays a central role in activating the type I interferon response following viral infection. Consequently, many viruses are known to target IRF-3 to inhibit the type I interferon response pathway (2, 13, 26, 45, 50). Viral infection results in the phosphorylation of IRF-3 at specific serine residues in the C terminus (25, 57, 61). Phosphorylated IRF-3 forms a homodimer, translocates to the nucleus, and associates with the transcriptional coactivator p300/CBP prior to binding to target DNA elements and inducing transcription (48, 59). In view of this, we investigated the phosphorylation and dimerization status of IRF-3 in RV14-infected HeLa cells.

Work in other laboratories has shown that phosphorylation of IRF-3 results in the appearance of a slower-migrating form that is detectable by immunoblotting (25, 57). Analysis of lysates from RV14-infected cells revealed that a slower-migrating form of IRF-3 was detectable by 3 hpi and that by 7 hpi this was the predominant form of IRF-3 in infected cells (Fig. 3A). This slower-migrating band appeared to comigrate with the phosphorylated IRF-3 produced following poly(I:C) treatment (data not shown), suggesting that it did represent phosphorylated, activated IRF-3. It should be pointed out, however, that IRF-3 is phosphorylated at multiple sites in its C terminus in response to viral infection (25, 57, 61) and that, using our gel conditions, we were unable to resolve the different phosphorylated forms of IRF-3 that have been reported by others (44). Thus, there may be qualitative differences between IRF-3 in cells infected with RV14 and treated with poly(I:C).

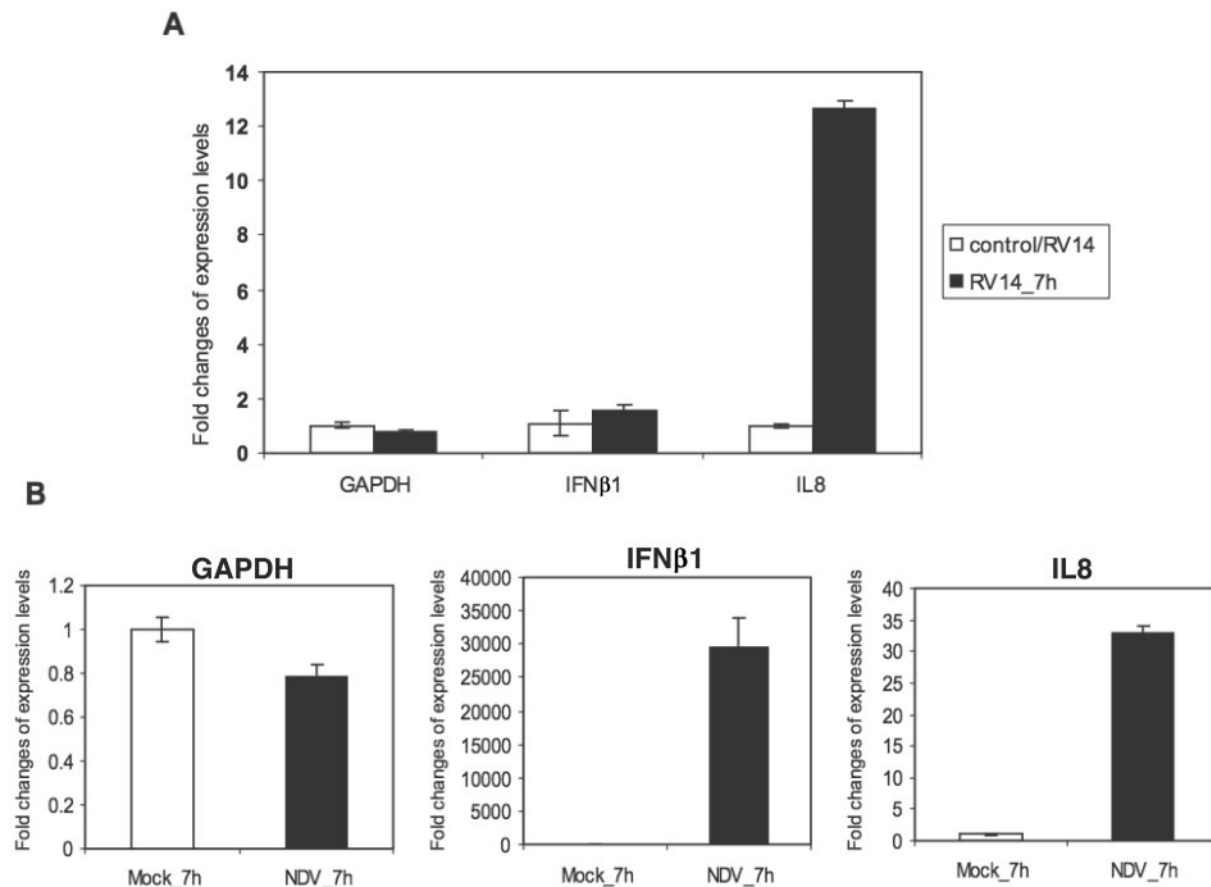


FIG. 4. Expression of IFN- $\beta$  mRNA and IL-8 mRNA in RV14-infected A549 cells. (A) Total RNAs extracted from mock-infected or RV14-infected cells were analyzed by qRT-PCR. qRT-PCR data for IFN- $\beta$  (IFN $\beta$ 1) and IL-8 (IL8) mRNA are shown, with error bars indicating one standard deviation from the results from three replicates. Results for GAPDH are shown as a normalization control. (B) Total RNAs extracted from mock-infected or NDV-infected A549 cells for the indicated time were analyzed by qRT-PCR. IFN- $\beta$ , IL-8, and GAPDH mRNAs were examined as described for panel A.

To determine if RV14 infection might interfere with dimerization of IRF-3, we examined the status of IRF-3 by native PAGE, followed by immunoblotting. Under these conditions, dimerized IRF-3 has significantly retarded mobility compared to that of monomeric IRF-3 (19). Analysis of lysates from RV14-infected cells revealed that by 7 hpi only a very small amount of IRF-3 dimer had formed (Fig. 3B). In contrast, poly(I:C) treatment resulted in robust induction of IRF-3 dimerization (Fig. 3B). These results suggest that RV14 has in place a mechanism to inhibit dimerization of IRF-3 and thus prevent the induction of IFN- $\beta$  mRNA.

**RV14 inhibits dimerization of IRF-3 in A549 cells.** To further extend and confirm the biological relevance of these findings to RV14 pathogenesis, we have analyzed the status of IRF-3 and induction of the type I interferon response in RV14-infected A549 lung alveolar epithelial cells. First, we examined IFN- $\beta$  mRNA levels in RV14-infected A549 cells by qRT-PCR. The results demonstrate that RV14 infection fails to induce detectable levels of IFN- $\beta$  mRNA in A549 cells (Fig. 4A). Analysis of these same RNA samples revealed strong induction of IL-8 mRNA, as has been reported by others (47, 51, 63). As a positive control for induction of IFN- $\beta$  mRNA, we infected A549 cells with Newcastle disease virus (NDV). Infection

with NDV results in an increase in IFN- $\beta$  mRNA levels of more than 25,000-fold over those of the mock-infected controls (Fig. 4B). These results indicate that infection of A549 alveolar epithelial cells with RV14 does not result in the accumulation of IFN- $\beta$  mRNA.

We next determined if infection of A549 cells with RV14 resulted in changes to the subcellular distribution and phosphorylation of IRF-3 similar to those seen in HeLa cells. Analysis of IRF-3 subcellular localization in RV14-infected A549 cells by immunofluorescence assay showed that by 3 hpi IRF-3 is predominantly nuclear, indicating that it is translocated to the nucleus following infection (Fig. 5A). Treatment of A549 cells with poly(I:C) resulted in a similar increase in nuclear staining (data not shown). Analysis of the phosphorylation status indicated that IRF-3 is phosphorylated in RV14-infected A549 cells, as was evidenced by the increased intensity of the slower-migrating form of IRF-3 detected at 4 hpi, 5 hpi, and 7 hpi (Fig. 5B). Analysis of A549 cells treated with poly(I:C) also indicated a similar increase in the intensity of the slower-migrating form of IRF-3 (data not shown). These results indicate that RV14 infection can trigger the nuclear translocation and phosphorylation of IRF-3 in both A549 and HeLa cells.

To determine if dimerization of IRF-3 occurred in RV14-

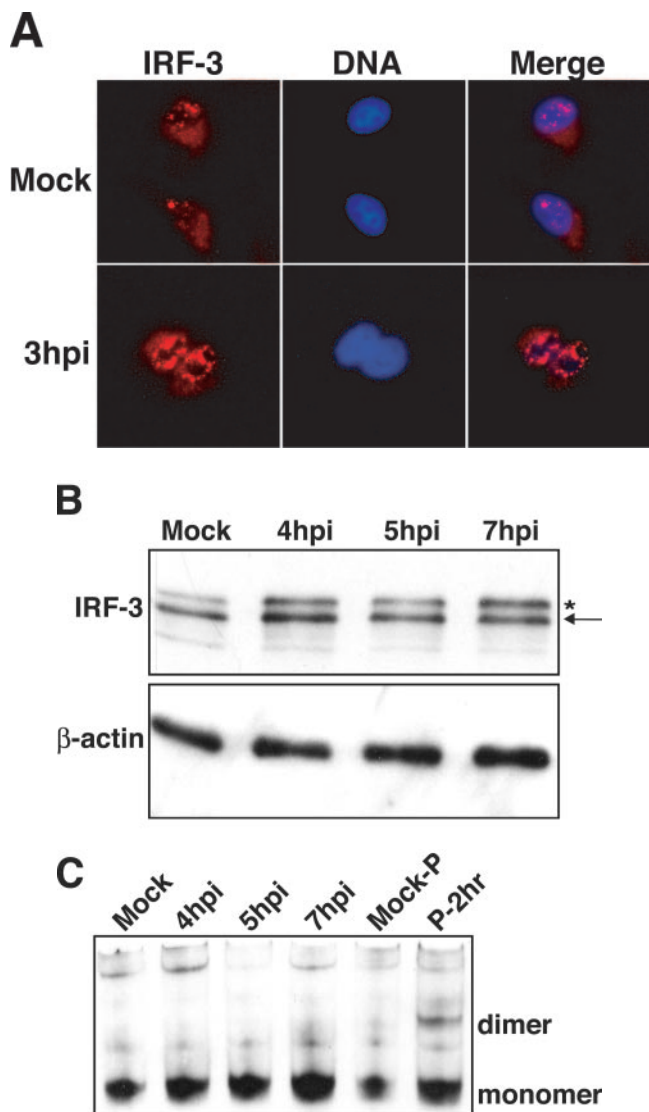


FIG. 5. Analysis of the status of IRF-3 in RV14-infected A549 cells. (A) Subcellular localization of IRF-3. A549 cells were either mock infected or infected with RV14 for the indicated amount of time and were analyzed by immunofluorescence assay. The IRF-3 panels show cells stained with a rabbit polyclonal antibody to detect IRF-3, using a tetramethyl rhodamine isothiocyanate filter. The DNA panels show the same field stained with Hoechst to reveal nuclei. The merged panels show overlays of the IRF-3 and DNA images. (B) Phosphorylation of IRF-3. Whole-cell lysates prepared from mock-infected cells or cells that had been infected with RV14 for the indicated amounts of time were analyzed by immunoblotting. IRF-3 was detected by probing the membrane with rabbit polyclonal antibody that detects human IRF-3. The nonphosphorylated form of IRF-3 is indicated with an arrow, and the phosphorylated form is indicated with an asterisk. The membrane was stripped and reprobed with an antibody to  $\beta$ -actin to show equivalent loading of protein lysates. (C) Homodimerization of IRF-3. Cell lysates prepared from mock-infected cells or cells that had been infected with RV14 or treated with poly(I:C) for the indicated amounts of time were analyzed by native PAGE, followed by immunoblotting to detect IRF-3. The monomeric and dimeric forms of IRF-3 are indicated.

infected A549 cells, we analyzed whole-cell lysates by native PAGE, followed by immunoblotting. The results indicated a lack of detectable levels of IRF-3 homodimer in RV14-infected A549 cells, even at 7 hpi (Fig. 5C). In contrast, analysis of A549 cells treated with poly(I:C) showed a robust induction of IRF-3 homodimer formation (Fig. 5C). In summary, these results indicate that RV14 infection of HeLa and A549 cells results in the nuclear translocation and phosphorylation of IRF-3 without the appearance of homodimers or the induction of IFN- $\beta$  mRNA synthesis.

**Inhibition of dsRNA response by RV14.** Poly(I:C) is a synthetic analogue of double-stranded RNA (dsRNA), as evidenced by the activation of IRF-3 and the induction of IFN- $\beta$  mRNA (37, 57, 61). Interestingly, Dodd and Kirkegaard found that infection with poliovirus inhibits the ability of cells to produce IFN- $\beta$  mRNA in response to treatment with poly(I:C) (11; K. Kirkegaard and D. Dodd, personal communications). In addition, Richtsteiger et al. reported that infection of cells with coxsackievirus B3 followed by poly(I:C) treatment resulted in 32% inhibition of IFN- $\beta$  mRNA induction compared to that in cells treated with poly(I:C) alone (38). To determine if infection with RV14 can similarly inhibit the induction of IFN- $\beta$ , HeLa cells were infected with RV14 and then treated with poly(I:C) at 1.5 hpi for an additional 2.5 h. qRT-PCR analysis of mock-infected HeLa cells treated with poly(I:C) for 2.5 h resulted in a 180-fold increase in IFN- $\beta$  mRNA levels (Fig. 6A). In contrast, qRT-PCR analysis of total RNA isolated from infected cells that had been treated with poly(I:C) revealed only a 37-fold induction of IFN- $\beta$  mRNA (Fig. 6A). This represents an 80% reduction in the levels of IFN- $\beta$  mRNA induction by poly(I:C) treatment in infected cells compared to those in uninfected cells (Fig. 6A). Similarly, comparison of IFN- $\beta$  mRNA induction by poly(I:C) in uninfected or RV14-infected A549 cells revealed that RV14 resulted in a 50% inhibition of IFN- $\beta$  mRNA levels (Fig. 7A). Conversely, RV14 infection did not interfere with the induction of IL-8 following poly(I:C) treatment in either HeLa or A549 cells (Fig. 6B and 7B). These results indicate that RV14 encodes a mechanism that can specifically prevent the induction of IFN- $\beta$  mRNA synthesis caused by poly(I:C) treatment.

Since very little dimerization of IRF-3 was observed in RV14-infected HeLa and A549 cells (Fig. 3B and 5C), we wanted to determine if the inhibition of IFN- $\beta$  mRNA induction in poly(I:C)-treated cells could be explained by a lack of dimerized IRF-3. Analysis of lysates from uninfected or RV14-infected cells treated with poly(I:C) revealed that dimerization of IRF-3 was reduced by 35% in HeLa cells (Fig. 8) and 17% in A549 cells (data not shown). These results indicate that, although reduced in abundance, IRF-3 homodimers do form in RV14-infected cells treated with poly(I:C). Currently it is not clear if the reduction in IRF-3 dimer levels is sufficient to account for the 80% and 50% inhibition of IFN- $\beta$  mRNA levels in HeLa and A549 cells, respectively. Alternatively, these results could indicate that RV14 encodes another activity that can inhibit IFN- $\beta$  mRNA synthesis in poly(I:C)-treated cells independently of IRF-3 dimerization status.

## DISCUSSION

In this study, we have examined the host response to RV14 infection, with particular attention focused on the type I IFN

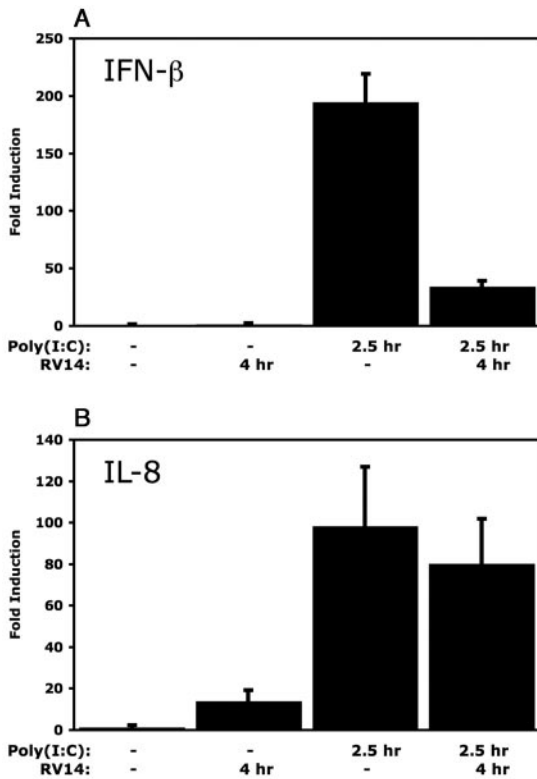


FIG. 6. Inhibition of the dsRNA response in HeLa cells. (A) IFN- $\beta$  mRNA levels. HeLa cells were either mock infected or infected with RV14 and then treated with poly(I:C) or not for the indicated amounts of time. Total RNA was isolated and analyzed by qRT-PCR for IFN- $\beta$  mRNA and normalized to levels of rRNA. Error bars indicate one standard deviation from the results from three biological replicates. (B) The RNAs described above were analyzed by qRT-PCR to determine IL-8 mRNA levels.

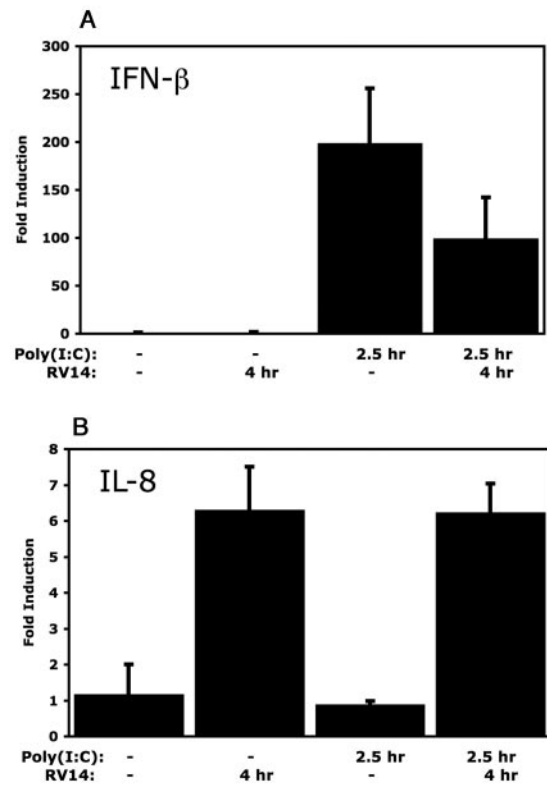


FIG. 7. Inhibition of the dsRNA response in A549 cells. (A) IFN- $\beta$  mRNA levels. A549 cells were either mock infected or infected with RV14 and then treated with poly(I:C) or not for the indicated amounts of time. Total RNA was isolated and analyzed by qRT-PCR for IFN- $\beta$  mRNA and normalized to levels of rRNA. Error bars indicate one standard deviation from the results from three biological replicates. (B) The RNAs described above were analyzed by qRT-PCR to determine IL-8 mRNA levels.

response and activation of IRF-3. The results demonstrate that, although RV14 infection results in altered levels of a wide variety of host mRNAs, production of IFN- $\beta$  or activation of the Jak/STAT pathway is not seen. IRF-3 is apparently activated, as it appeared to be phosphorylated and showed nuclear accumulation in RV14-infected cells. However, despite IRF-3 phosphorylation and nuclear translocation, very little dimerization of IRF-3 was detected in infected cells. Analysis of A549 cells extended these findings to a lung alveolar epithelial cell line and indicates that these results are not unique to HeLa cells. Collectively, these results demonstrate that host cells respond to RV14 infection by initiating a type I interferon response but that RV14 has an ability to prevent the dimerization of IRF-3 and thus inhibit the induction of IFN- $\beta$  mRNA.

Although early experiments by Stoker et al. demonstrated that tissue culture cells infected with rhinovirus produce little type I interferon (46), recent experiments indicate that this may not always be the case. Examination of primary bronchial epithelial cells from healthy individuals revealed that significant amounts of IFN- $\beta$  mRNA and protein were produced following infection with RV16 (9, 56). In contrast, very little IFN- $\beta$  was produced when bronchial epithelial cells from asthmatic individuals were infected with RV16 (56). Currently, it is

not clear if the differences between the results presented here and those described above are due to differences between serotypes or to the use of primary versus immortalized cell lines. One interesting possibility is that HeLa and A549 cells may more closely reflect the environment found in bronchial epithelial cells from asthmatic individuals.

Dodd and Kirkegaard found that infection with poliovirus inhibits the ability of cells to produce IFN- $\beta$  mRNA in re-

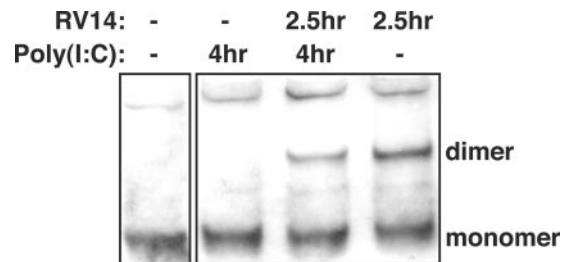


FIG. 8. IRF-3 homodimerization in cells treated with poly(I:C). Whole-cell lysates were prepared from cells that were either mock infected or infected with RV14 and then treated with poly(I:C) or not for the indicated amounts of time. Lysates were analyzed by native PAGE, followed by immunoblotting to detect IRF-3. The monomeric and dimeric forms of IRF-3 are indicated.

sponse to treatment with dsRNA (11; K. Kirkegaard and D. Dodd, personal communications). Recent work by Neznanov et. al (31) has provided a potential explanation for the lack of IFN- $\beta$  mRNA in poliovirus-infected cells. These authors found that during poliovirus infection the p65/RelA subunit of NF- $\kappa$ B is cleaved by the 3C protease. Thus, it is possible that targeted degradation of p65/RelA in poliovirus-infected cells may contribute to the inhibition of IFN- $\beta$  mRNA synthesis. This same study demonstrated that p65/RelA was targeted for degradation in RV14-infected cells, although levels of p65/RelA were not altered until 8 hpi (31). The results presented above, along with numerous prior studies documenting strong transcriptional induction of NF- $\kappa$ B-responsive promoters at early times in RV14-infected cells (22, 34, 35, 63, 64), suggest that inactivation of NF- $\kappa$ B cannot explain the lack of IFN- $\beta$  mRNA production in RV14-infected cells.

The importance of the type I interferon response in the host defense against viral infection is perhaps best illustrated by the variety of mechanisms viruses have evolved to counteract it. Interestingly, most of these mechanisms target early events in this response that prevent the activation of IRF-3 (3, 4, 7, 13, 26, 39, 54). In contrast, attenuation of this response following activation of IRF-3 is less common. Bunyamwera virus, a negative-stranded RNA virus, prevents the expression of IFN- $\beta$  mRNA despite the nuclear translocation of IRF-3 (23, 58). This requires the viral nonstructural protein, NSs, which has recently been shown to cause a general inhibition of mRNA synthesis by preventing phosphorylation of the C-terminal domain of RNA polymerase II (52, 58). The microarray results presented here, along with work from a number of laboratories (12, 35, 41, 47, 49, 51, 63, 64), demonstrate that a variety of cellular promoters are activated in infected cells and indicate that RV14 infection does not result in a global inhibition of transcription.

Interestingly, it was recently reported that IRF-3 is translocated to the nucleus after infection with the severe acute respiratory syndrome coronavirus (SARS-coV) (45). In this study, the authors found that the translocated IRF-3 did not form homodimers or associate with the transcriptional coactivator CBP. However, unlike what we observed in RV14-infected cells, IRF-3 was not phosphorylated in cells infected with SARS-coV (45). Thus, it appears that, while SARS-coV is able to prevent phosphorylation of IRF-3 and hence transcriptional activation, rhinovirus is able to prevent dimerization despite triggering phosphorylation. Similarly, infection with a naturally occurring noncytopathogenic variant of bovine viral diarrhea virus (ncpBVDV) has also been shown to inhibit IFN- $\beta$  mRNA synthesis, despite nuclear translocation of IRF-3 (2, 42). However, as phosphorylation and dimerization of IRF-3 in ncpBVDV-infected cells was not examined, it is unclear if RV14 and ncpBVDV inhibit IRF-3 activation by similar mechanisms.

By inhibiting dimerization, RV prevents the formation of the IRF-3 holocomplex consisting of dimerized IRF-3 associated with CBP/p300 and, thus, induction of IFN- $\beta$  mRNA. Currently, the mechanism by which RV14 prevents IRF-3 dimerization is not known. The C terminus of IRF-3 contains six serine residues that are potential sites of phosphorylation (25, 57, 61). These serine residues can be grouped into two clusters: S385/386 and S396/398/402/405. Servant

et al. showed that S396 was phosphorylated in response to Sendai virus infection and treatment with dsRNA (43). More recently, it was found that, following infection with Newcastle disease virus, only the dimeric form of IRF-3 was phosphorylated at S386 and that mutation of this residue abolished dimerization (30). Our analysis of IRF-3 did not allow us to distinguish between phosphorylation at one or both of these sites in RV14-infected cells. Thus, one possibility is that RV14 selectively inhibits phosphorylation of certain residues while allowing phosphorylation of others. If this scenario is correct, then it seems likely that phosphorylation of S386 is inhibited due to its requirement for dimerization (30). Experiments are under way to further delineate the mechanism(s) by which RV14 inhibits IRF-3 homodimerization and to identify the viral factor(s) responsible.

#### ACKNOWLEDGMENTS

We thank Karla Kirkegaard and Dana Dodd for sharing results prior to publication, for many helpful discussions and advice, and for critical readings of the manuscript; Takashi Fujita and Nancy Reich for providing reagents and advice; Gustavo Arrizabalaga for helpful discussions; and the groups of Peter Palese and Adolfo Garcia-Sastre for constructive criticism in the early stages of this work.

K.E.G. was supported by NIH grants from the NCCR Center of Biomedical Research Excellence (P20 RR15587) and Biomedical Research Infrastructure Network program (P20 RR016454). R.E.B. and T.P. are supported by NIH NIAID grant 5P01AI052106. R.E.B.'s bioinformatics infrastructure study is supported by NIH NCCR grant 1S10RR019423.

#### REFERENCES

1. Abzug, M. J., A. C. Beam, E. A. Gyorkos, and M. J. Levin. 1990. Viral pneumonia in the first month of life. *Pediatr. Infect. Dis. J.* **9**:881–885.
2. Baigent, S. J., G. Zhang, M. D. Fray, H. Flick-Smith, S. Goodbourn, and J. W. McCauley. 2002. Inhibition of beta interferon transcription by noncytopathogenic bovine viral diarrhea virus is through an interferon regulatory factor 3-dependent mechanism. *J. Virol.* **76**:8979–8988.
3. Barro, M., and J. T. Patton. 2005. Rotavirus nonstructural protein 1 subverts innate immune response by inducing degradation of IFN regulatory factor 3. *Proc. Natl. Acad. Sci. USA* **102**:4114–4119.
4. Basler, C. F., A. Mikulasova, L. Martinez-Sobrido, J. Paragas, E. Muhlberger, M. Bray, H. D. Klenk, P. Palese, and A. Garcia-Sastre. 2003. The Ebola virus VP35 protein inhibits activation of interferon regulatory factor 3. *J. Virol.* **77**:7945–7956.
5. Bertino, J. S. 2002. Cost burden of viral respiratory infections: issues for formulary decision makers. *Am. J. Med.* **112**(Suppl. 6A):42S–49S.
6. Biron, A. B., and G. C. Sen. 2001. Interferons and other cytokines, p. 321–351. *In* B. N. Fields and D. M. Knipe (ed.), *Fields virology*, 4th ed. Lippincott Williams & Wilkins, Philadelphia, Pa.
7. Bossert, B., S. Marozin, and K. K. Conzelmann. 2003. Nonstructural proteins NS1 and NS2 of bovine respiratory syncytial virus block activation of interferon regulatory factor 3. *J. Virol.* **77**:8661–8668.
8. Browne, E. P., B. Wing, D. Coleman, and T. Shenk. 2001. Altered cellular mRNA levels in human cytomegalovirus-infected fibroblasts: viral block to the accumulation of antiviral mRNAs. *J. Virol.* **75**:12319–12330.
9. Chen, Y., E. Hamati, P. K. Lee, W. M. Lee, S. Wachi, D. Schnurr, S. Yagi, G. Dolganov, H. Boushey, P. Avila, and R. Wu. 2005. Rhinovirus induces airway epithelial gene expression through dsRNA and interferon-dependent pathways. *Am. J. Respir. Cell Mol. Biol.* **34**:192–203.
10. Couch, R. B. 2001. Rhinoviruses, p. 777–798. *In* B. N. Fields and D. M. Knipe (ed.), *Fields virology*, 4th ed. Lippincott Williams & Wilkins, Philadelphia, Pa.
11. Dodd, D. A. 2002. Effects of poliovirus infection and picornaviral 3A proteins on the cellular response to viral infection. Ph.D. thesis. Stanford University, Stanford, Calif.
12. Einarsson, O., G. P. Geba, Z. Zhu, M. Landry, and J. A. Elias. 1996. Interleukin-11: stimulation in vivo and in vitro by respiratory viruses and induction of airways hyperresponsiveness. *J. Clin. Investig.* **97**:915–924.
13. Foy, E., K. Li, C. Wang, R. Sumpter, Jr., M. Ikeda, S. M. Lemon, and M. Gale, Jr. 2003. Regulation of interferon regulatory factor-3 by the hepatitis C virus serine protease. *Science* **300**:1145–1148.
14. Garofalo, R., F. Mei, R. Espejo, G. Ye, H. Haeblerle, S. Baron, P. L. Ogra, and V. E. Reyes. 1996. Respiratory syncytial virus infection of human respi-

- ratory epithelial cells up-regulates class I MHC expression through the induction of IFN-beta and IL-1 alpha. *J. Immunol.* **157**:2506–2513.
15. Geiss, G. K., V. S. Carter, Y. He, B. K. Kwiciszewski, T. Holzman, M. J. Korth, C. A. Lazaro, N. Fausto, R. E. Bumgarner, and M. G. Katze. 2003. Gene expression profiling of the cellular transcriptional network regulated by alpha/beta interferon and its partial attenuation by the hepatitis C virus nonstructural 5A protein. *J. Virol.* **77**:6367–6375.
  16. Ghosh, S., R. Champlin, R. Couch, J. Englund, I. Raad, S. Malik, M. Luna, and E. Whimbey. 1999. Rhinovirus infections in myelosuppressed adult blood and marrow transplant recipients. *Clin. Infect. Dis.* **29**:528–532.
  17. Gustin, K. E., and P. Sarnow. 2002. Inhibition of nuclear import and alteration of nuclear pore complex composition by rhinovirus. *J. Virol.* **76**:8787–8796.
  18. Hall, D. J., M. E. Bates, L. Guar, M. Cronan, N. Korpi, and P. J. Bertics. 2005. The role of p38 MAPK in rhinovirus-induced monocyte chemoattractant protein-1 production by monocytic-lineage cells. *J. Immunol.* **174**:8056–8063.
  19. Iwamura, T., M. Yoneyama, K. Yamaguchi, W. Suhara, W. Mori, K. Shiota, Y. Okabe, H. Namiki, and T. Fujita. 2001. Induction of IRF-3/-7 kinase and NF- $\kappa$ B in response to double-stranded RNA and virus infection: common and unique pathways. *Genes Cells* **6**:375–388.
  20. Jamaluddin, M., S. Wang, R. P. Garofalo, T. Elliott, A. Casola, S. Baron, and A. R. Brasier. 2001. IFN- $\beta$  mediates coordinate expression of antigen-processing genes in RSV-infected pulmonary epithelial cells. *Am. J. Physiol. Lung Cell. Mol. Physiol.* **280**:L248–L257.
  21. Johnston, S. L., P. K. Pattemore, G. Sanderson, S. Smith, F. Lampe, L. Josephs, P. Symington, S. O'Toole, S. H. Myint, D. A. Tyrrell, et al. 1995. Community study of role of viral infections in exacerbations of asthma in 9–11 year old children. *BMJ* **310**:1225–1229.
  22. Kim, J., S. P. Sanders, E. S. Sikierski, V. Casolaro, and D. Proud. 2000. Role of NF-kappa B in cytokine production induced from human airway epithelial cells by rhinovirus infection. *J. Immunol.* **165**:3384–3392.
  23. Kohl, A., R. F. Clayton, F. Weber, A. Bridgen, R. E. Randall, and R. M. Elliott. 2003. Bunyamwera virus nonstructural protein NSs counteracts interferon regulatory factor 3-mediated induction of early cell death. *J. Virol.* **77**:7999–8008.
  24. Kumar, K. P., K. M. McBride, B. K. Weaver, C. Dingwall, and N. C. Reich. 2000. Regulated nuclear-cytoplasmic localization of interferon regulatory factor 3, a subunit of double-stranded RNA-activated factor 1. *Mol. Cell. Biol.* **20**:4159–4168.
  25. Lin, R., C. Heylbroeck, P. M. Pitha, and J. Hiscott. 1998. Virus-dependent phosphorylation of the IRF-3 transcription factor regulates nuclear translocation, transactivation potential, and proteasome-mediated degradation. *Mol. Cell. Biol.* **18**:2986–2996.
  26. Lin, R., R. S. Noyce, S. E. Collins, R. D. Everett, and K. L. Mossman. 2004. The herpes simplex virus ICP0 RING finger domain inhibits IRF3- and IRF7-mediated activation of interferon-stimulated genes. *J. Virol.* **78**:1675–1684.
  27. Loveys, D. A., S. Kulkarni, and P. L. Atreya. 2000. Role of type I IFNs in the in vitro attenuation of live, temperature-sensitive vaccine strains of human respiratory syncytial virus. *Virology* **271**:390–400.
  28. McMillan, J. A., L. B. Weiner, A. M. Higgins, and K. Macknight. 1993. Rhinovirus infection associated with serious illness among pediatric patients. *Pediatr. Infect. Dis. J.* **12**:321–325.
  29. Monto, A. S., A. M. Fendrick, and M. W. Sarnes. 2001. Respiratory illness caused by picornavirus infection: a review of clinical outcomes. *Clin. Ther.* **23**:1615–1627.
  30. Mori, M., M. Yoneyama, T. Ito, K. Takahashi, F. Inagaki, and T. Fujita. 2004. Identification of Ser-386 of interferon regulatory factor 3 as critical target for inducible phosphorylation that determines activation. *J. Biol. Chem.* **279**:9698–9702.
  31. Neznanov, N., K. M. Chumakov, L. Neznanova, A. Almasan, A. K. Banerjee, and A. V. Gudkov. 2005. Proteolytic cleavage of the p65-RelA subunit of NF- $\kappa$ B during poliovirus infection. *J. Biol. Chem.* **280**:24153–24158.
  32. Olson, M. O., K. Guetzow, and H. Busch. 1981. Localization of phosphoprotein C23 in nucleoli by immunological methods. *Exp. Cell Res.* **135**:259–265.
  33. Pahl, H. L. 1999. Activators and target genes of Rel/NF-kappaB transcription factors. *Oncogene* **18**:6853–6866.
  34. Papi, A., and S. L. Johnston. 1999. Respiratory epithelial cell expression of vascular cell adhesion molecule-1 and its up-regulation by rhinovirus infection via NF- $\kappa$ B and GATA transcription factors. *J. Biol. Chem.* **274**:30041–30051.
  35. Papi, A., and S. L. Johnston. 1999. Rhinovirus infection induces expression of its own receptor intercellular adhesion molecule 1 (ICAM-1) via increased NF- $\kappa$ B-mediated transcription. *J. Biol. Chem.* **274**:9707–9720.
  36. Peng, T., T. R. Golub, and D. M. Sabatini. 2002. The immunosuppressant rapamycin mimics a starvation-like signal distinct from amino acid and glucose deprivation. *Mol. Cell. Biol.* **22**:5575–5584.
  37. Raj, N. B., and P. M. Pitha. 1980. The messenger RNA sequences in human fibroblast cells induced with poly rI: C to produce interferon. *Nucleic Acids Res.* **8**:3427–3437.
  38. Richtsteiger, R., C. Henke-Gendo, M. Schmidtke, G. Harste, and A. Heim. 2003. Quantitative multiplex real-time PCR for the sensitive detection of interferon beta gene induction and viral suppression of interferon beta expression. *Cytokine* **24**:190–200.
  39. Ronco, L. V., A. Y. Karpova, M. Vidal, and P. M. Howley. 1998. Human papillomavirus 16 E6 oncoprotein binds to interferon regulatory factor-3 and inhibits its transcriptional activity. *Genes Dev.* **12**:2061–2072.
  40. Samuel, C. E. 2001. Antiviral actions of interferons. *Clin. Microbiol. Rev.* **14**:778–809.
  41. Schroth, M. K., E. Grimm, P. Frindt, D. M. Galagan, S. I. Konno, R. Love, and J. E. Gern. 1999. Rhinovirus replication causes RANTES production in primary bronchial epithelial cells. *Am. J. Respir. Cell Mol. Biol.* **20**:1220–1228.
  42. Schweizer, M., and E. Peterhans. 2001. Noncytopathic bovine viral diarrhea virus inhibits double-stranded RNA-induced apoptosis and interferon synthesis. *J. Virol.* **75**:4692–4698.
  43. Servant, M. J., N. Grandvaux, B. R. tenOever, D. Duguay, R. Lin, and J. Hiscott. 2003. Identification of the minimal phosphoacceptor site required for in vivo activation of interferon regulatory factor 3 in response to virus and double-stranded RNA. *J. Biol. Chem.* **278**:9441–9447.
  44. Servant, M. J., B. ten Oever, C. LePage, L. Conti, S. Gessani, I. Julkunen, R. Lin, and J. Hiscott. 2001. Identification of distinct signaling pathways leading to the phosphorylation of interferon regulatory factor 3. *J. Biol. Chem.* **276**:355–363.
  45. Spiegel, M., A. Pichlmair, L. Martinez-Sobrido, J. Cros, A. Garcia-Sastre, O. Haller, and F. Weber. 2005. Inhibition of beta interferon induction by severe acute respiratory syndrome coronavirus suggests a two-step model for activation of interferon regulatory factor 3. *J. Virol.* **79**:2079–2086.
  46. Stoker, D., J. Kiernat, and C. Gauntt. 1973. Interferon induction by rhinoviruses and effect of interferon on rhinovirus yields in human cell lines. *Proc. Soc. Exp. Biol. Med.* **143**:23–27.
  47. Subauste, M. C., D. B. Jacoby, S. M. Richards, and D. Proud. 1995. Infection of a human respiratory epithelial cell line with rhinovirus. Induction of cytokine release and modulation of susceptibility to infection by cytokine exposure. *J. Clin. Investig.* **96**:549–557.
  48. Suhara, W., M. Yoneyama, I. Kitabayashi, and T. Fujita. 2002. Direct involvement of CREB-binding protein/p300 in sequence-specific DNA binding of virus-activated interferon regulatory factor-3 holocomplex. *J. Biol. Chem.* **277**:22304–22313.
  49. Suzuki, T., M. Yamaya, M. Kamanaka, Y. X. Jia, K. Nakayama, M. Hosoda, N. Yamada, H. Nishimura, K. Sekizawa, and H. Sasaki. 2001. Type 2 rhinovirus infection of cultured human tracheal epithelial cells: role of LDL receptor. *Am. J. Physiol. Lung Cell. Mol. Physiol.* **280**:L409–L420.
  50. Talon, J., C. M. Horvath, R. Polley, C. F. Basler, T. Muster, P. Palese, and A. Garcia-Sastre. 2000. Activation of interferon regulatory factor 3 is inhibited by the influenza A virus NS1 protein. *J. Virol.* **74**:7989–7996.
  51. Terajima, M., M. Yamaya, K. Sekizawa, S. Okinaga, T. Suzuki, N. Yamada, K. Nakayama, Y. Ohru, T. Oshima, Y. Numazaki, and H. Sasaki. 1997. Rhinovirus infection of primary cultures of human tracheal epithelium: role of ICAM-1 and IL-1beta. *Am. J. Physiol.* **273**:L749–L759.
  52. Thomas, D., G. Blakqori, V. Wagner, M. Banholzer, N. Kessler, R. M. Elliott, O. Haller, and F. Weber. 2004. Inhibition of RNA polymerase II phosphorylation by a viral interferon antagonist. *J. Biol. Chem.* **279**:31471–31477.
  53. Turner, R. B. 2001. The treatment of rhinovirus infections: progress and potential. *Antivir. Res.* **49**:1–14.
  54. Unterstab, G., S. Ludwig, A. Anton, O. Planz, B. Dauber, D. Krappmann, G. Heins, C. Ehrhardt, and T. Wolff. 2005. Viral targeting of the interferon- $\beta$ -inducing Traf family member-associated NF- $\kappa$ B activator (TANK)-binding kinase-1. *Proc. Natl. Acad. Sci. USA* **102**:13640–13645.
  55. van Dam, H., D. Wilhelm, I. Herr, A. Steffen, P. Herrlich, and P. Angel. 1995. ATF-2 is preferentially activated by stress-activated protein kinases to mediate c-jun induction in response to genotoxic agents. *EMBO J.* **14**:1798–1811.
  56. Wark, P. A., S. L. Johnston, F. Bucchieri, R. Powell, S. Puddicombe, V. Laza-Stanca, S. T. Holgate, and D. E. Davies. 2005. Asthmatic bronchial epithelial cells have a deficient innate immune response to infection with rhinovirus. *J. Exp. Med.* **201**:937–947.
  57. Weaver, B. K., K. P. Kumar, and N. C. Reich. 1998. Interferon regulatory factor 3 and CREB-binding protein/p300 are subunits of double-stranded RNA-activated transcription factor DRAF1. *Mol. Cell. Biol.* **18**:1359–1368.
  58. Weber, F., A. Bridgen, J. K. Fazakerley, H. Streitenfeld, N. Kessler, R. E. Randall, and R. M. Elliott. 2002. Bunyamwera bunyavirus nonstructural protein NSs counteracts the induction of alpha/beta interferon. *J. Virol.* **76**:7949–7955.
  59. Yang, H., C. H. Lin, G. Ma, M. Orr, M. O. Baffi, and M. G. Wathelet. 2002. Transcriptional activity of interferon regulatory factor (IRF)-3 depends on multiple protein-protein interactions. *Eur. J. Biochem.* **269**:6142–6151.
  60. Yoneyama, M., W. Suhara, and T. Fujita. 2002. Control of IRF-3 activation by phosphorylation. *J. Interferon Cytokine Res.* **22**:73–76.
  61. Yoneyama, M., W. Suhara, Y. Fukuhara, M. Fukuda, E. Nishida, and T.

- Fujita.** 1998. Direct triggering of the type I interferon system by virus infection: activation of a transcription factor complex containing IRF-3 and CBP/p300. *EMBO J.* **17**:1087–1095.
62. **Zhang, Y., B. A. Luxon, A. Casola, R. P. Garofalo, M. Jamaluddin, and A. R. Brasier.** 2001. Expression of respiratory syncytial virus-induced chemokine gene networks in lower airway epithelial cells revealed by cDNA microarrays. *J. Virol.* **75**:9044–9058.
63. **Zhu, Z., W. Tang, J. M. Gwaltney, Jr., Y. Wu, and J. A. Elias.** 1997. Rhinovirus stimulation of interleukin-8 in vivo and in vitro: role of NF-kappaB. *Am. J. Physiol.* **273**:L814–L824.
64. **Zhu, Z., W. Tang, A. Ray, Y. Wu, O. Einarsson, M. L. Landry, J. Gwaltney, Jr., and J. A. Elias.** 1996. Rhinovirus stimulation of interleukin-6 in vivo and in vitro. Evidence for nuclear factor kappa B-dependent transcriptional activation. *J. Clin. Investig.* **97**:421–430.